ELSEVIER

Polymer 43 (2002) 2279–2286

polymer

www.elsevier.com/locate/polymer

Correlated electrical conductivity and mechanical property analysis of high-density polyethylene filled with graphite and carbon fiber

Wiriya Thongruang[a,1], Richard J. Spontak[a,b], C. Maurice Balik[a,*]

[a]*Department of Materials Science and Engineering, North Carolina State University, Raleigh, NC 27695, USA*
[b]*Department of Chemical Engineering, North Carolina State University, Raleigh, NC 27695, USA*

Received 5 July 2001; received in revised form 27 December 2001; accepted 31 December 2001

Abstract

The development of conductive polymer composites remains an important endeavor in light of growing energy concerns. In the present work, graphite (G), carbon fiber (CF) and G/CF mixtures are added to high-density polyethylene (HDPE) to discern if mixed fillers afford appreciable advantages over single fillers. The effects of filler type and composition on electrical conductivity, composite morphology and mechanical properties have been examined and correlated to establish structure–property relationships. The threshold loading levels required for G and CF to achieve measurable conductivity in HDPE have been identified. Addition of CF to HDPE/G composites is found to increase the conductivity relative to that of HDPE/G composites at the same filler concentration. This observed increase depends on CF length and becomes more pronounced at and beyond the threshold loading of the HDPE/G composite. Scanning electron microscopy is employed to elucidate the morphology of these multicomponent composites, whereas dynamic mechanical analysis reveals that filler concentration, composition and CF length impact both the magnitude and temperature dependence of the dynamic storage modulus. © 2002 Published by Elsevier Science Ltd.

Keywords: High-density polyethylene; Polymer composite; Electrical conductivity

1. Introduction

Carbonaceous fillers are regularly employed in the production of polymer composites to enhance electrical conductivity and mechanical properties, as well as to maintain light weight and corrosion resistance. Conductive carbonaceous fillers of current commercial relevance include carbon black (CB), graphite (G) and carbon fiber (CF), which differ greatly in both structure and form. Conductive polymer composites are used in a wide variety of industrial applications such as battery and fuel cell electrodes, antistatic media and corrosion-resistant materials. Consider, for example, the utility of CB particles, which have been routinely added to polyethylene (PE) and other polymers over the past quarter century for four main purposes: improved electrical conductivity, mechanical properties, color and UV stability [1–6]. Miyasaka et al. [7] report that the conductivity of PE/CB composites jumps by as much as 10 orders of magnitude at a critical concentration of CB, which they designate as the threshold concentration for CB percolation [8–10]. Since 1990, numerous studies [11–30] have investigated PE/CB composites to identify the factors responsible for improved electrical and mechanical properties. While we have focused exclusively on PE/CB composites here, the electrical properties of other polymers have also been improved through the addition of CB [31–35].

Graphite is another carbonaceous filler that has been incorporated into PE for electrical conductivity purposes [36]. The electron transport mechanism in PE/G composites has been examined [37] by d.c. conductivity analysis. Deviation from percolation theory at low graphite concentrations has been attributed to tunneling conduction between adjacent particles. Addition of G to thermoplastics generally combines the electrical properties of G with ease of processing, and may likewise promote attractive electrochemical, physical, mechanical and economic considerations [38]. Navarro-Laboulais et al. [39] have added G to high-density polyethylene (HDPE) and have applied percolation theory to study the impedance and resistance of their HDPE/G composites. Yi et al. [40] have demonstrated that the current–voltage behavior of HDPE/G composites is

---

[*] Corresponding author. Tel.: +1-919-515-2126; fax: +1-919-515-7724.
E-mail address: balik@ncsu.edu (C.M. Balik).

[1] Present address: Department of Mechanical Engineering, Prince of Songkla University, Hatyai, Songkla 90112, Thailand.

PII: S0032-3861(02)00043-5

non-ohmic regardless of G concentration and probe contact pressure. Since G is available in different sizes and shapes, the importance of these factors on conductivity has been investigated by Nagata et al. [41]. By modifying low-density polyethylene (LDPE) with both plate-like and spherical G, they have found that the conductivity of the LDPE/G composite with spherical G increases with decreasing particle size, while the conductivity of the composite with plate-like G increases linearly with increasing particle size. Song et al. [42] have also identified another non-negligible consideration in HDPE/G composites, namely the dependence of the self-heating temperature on the magnitude of the applied electric field.

High-aspect-ratio CF has also been added to polymers to enhance both electrical conductivity and mechanical reinforcement. In this case, however, CF length dispersity and composite anisotropy play crucial roles in property development [43]. In some cases, electrical and thermal conductivities have been found [44,45] to exhibit significant biaxial orientation due to the anisotropy of the CF. In such biaxially oriented CF composites, long fibers induce higher electrical conductivity. Short CFs blended with PVC, on the other hand, display excellent electrical properties at very low fiber concentrations ($\sim$1.0 phr) [46]. In polyester/CF composites, the conduction threshold concentration has been measured [47] to be 1–2 wt% CF.

These previous works have addressed polymer composites containing a single filler, mostly CB. This is due to the cost, small particle size (high surface area) and aggregation behavior of CB, the latter two of which are responsible for the relatively low loading levels needed to achieve desired conductivities. It is difficult, however, to prepare well-dispersed polymer/CB composites containing more than 35 wt% CB with simple mixing techniques. To overcome this limitation, Calleja et al. [48] have prepared HDPE composites with mixtures of CB and CF using conventional mixing and molding processes. In these samples, the CF provides charge transport over large distances, whereas the CB particles serve to improve interfiber points of contact. This synergy is illustrated in Fig. 1, which demonstrates that the connectivity of a G network is improved by adding CF to a polymer/G composite. Without CF, a higher concentration of G is needed to create a conductive path throughout the entire composite film. The present work is motivated by the lack of a systematic study of polymer composites composed of a mixture of G and CF, as well as by the difficulty of blending CB with polymers at high loading levels. Composites of HDPE, which is capable of resisting chemically aggressive environments in fuel cell applications, with G and CF fillers have been prepared for comparison with composites containing G/CF mixtures. The morphological features, electrical conductivity, mechanical and thermal properties of these conductive polymer composites are examined as functions of filler type, composition and concentration.

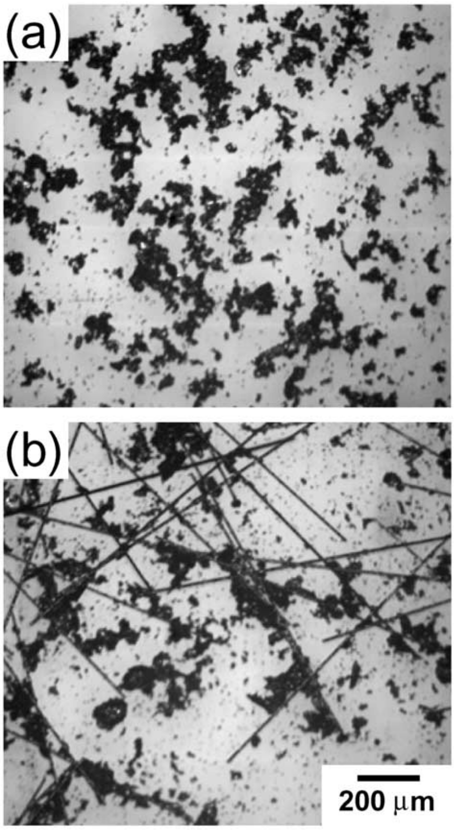

Fig. 1. Optical micrographs of (a) G and (b) G + CF filler particles spread randomly on a glass slide. The total filler mass is equal in both the figures. Addition of CF provides long conductive paths and improves the inter-particle contacts within the network.

2. Experimental

2.1. Materials

HDPE with M_w less than 200,000 g/mol was obtained in powder form from Celanese. Its melt flow index was measured as 7.52 g/10 min according to ASTM D1238. The mass density and melting temperature of this HDPE were 0.964 g/cm^3 and 134 °C, respectively, and the particle size range was 30–90 μm. Graphite (#4424) obtained from Asbury had a density of 2.24 g/cm^3 and an aggregate size of about 40 μm. Two types of polyacrylonitrile-derived CF identical in diameter (7.0 μm) and mass density (1.77–1.80 g/cm^3) but different in length (1.00 mm for CF$_1$ and 0.25 mm for CF$_2$) were obtained from Goodfellow. The volume resistivity of the CF was reported to be 1.5×10^{-3} Ωcm.

2.2. Preparation

The HDPE and fillers were first dry-mixed in a mechanical mixer to achieve a reasonably uniform dispersion, and then spread in a 40×120 mm^2 metal picture-frame mold with a thickness of either 0.2 or 0.5 mm (the bulk properties reported here are independent of sample thickness). The mold was placed in a Carver hydraulic press and heated to 170 °C. A pressure of 7.2 MPa was applied and held for 3 min to completely melt the HDPE. The mold was then cooled by circulating cold water through the platens. Composite films with filler loading levels up to 75% G or 20% CF were obtained by this process. Composites containing more than 20 wt% CF were visibly heterogeneous and therefore excluded from further consideration in this study.

2.3. Characterization

The electrical resistivity of 40×40 mm^2 sections of the molded films was measured at ambient temperature using the four-point probe technique (Veeco 5000) and correcting for sample geometry. The average resistivity of each specimen was obtained from seven repeated measurements at different locations on the specimen. Thermal properties of the HDPE in the composite films (including crystallinity, melting and crystallization temperatures) were discerned by differential scanning calorimetry (DSC, Perkin–Elmer DSC-7) at heating and cooling rates of 20 °C/min. The mechanical properties of the composite samples were investigated using dynamic mechanical analysis (DMA, TA Instruments DMA 983). The shear moduli and loss angle were measured at small strain amplitudes and a fixed frequency of 1.0 Hz in the linear viscoelastic regime. Composite samples measuring $13 \times 40 \times 0.5$ mm^3 were cut for DMA. Samples were annealed at 90 °C for 1 h prior to DMA and DSC analyses to ensure removal of residual stresses arising from molding and quenching. Variable-pressure scanning electron microscopy (SEM, Hitachi S-3200N) was used to ascertain the morphology of the composite films. Images were acquired from the sample surface in contact with the mold (after polishing) and from surfaces fractured in liquid nitrogen. To enhance the backscattered electron contrast between the HDPE matrix and the carbonaceous G, CF and G/CF fillers, specimens were stained with chlorosulfonic acid (HSO_3Cl), which selectively reacts with and stains the amorphous regions of HDPE [49,50]. An optical microscope (Olympus BH-2) equipped with a digital camera (Fuji HC-300Z) was used to discern the effects of composite film preparation on CF breakage in a limited number of HDPE/CF composites.

3. Results and discussion

3.1. Specimen uniformity and process reproducibility

Composite films of HDPE/G and HDPE/CF_1 at relatively high filler concentrations (50 and 75 wt% G, 15 wt% CF_1) have been cut in half, stacked and subsequently remolded to their original thickness to check on uniformity and process reproducibility using electrical conductivity as the measure of merit. Conductivity data collected from four repeated cut-stack-mold cycles are presented in Fig. 2 and reveal that the film with 50 wt% G exhibits very reproducible conductivity. Generally speaking, the HDPE/G composites visibly appear more uniform than those containing CF_1, as reflected by the size of the error bars included in Fig. 2. Higher loading levels of filler than those provided in Fig. 2 adversely affect film uniformity and process reproducibility, as discerned from both conductivity measurements and appearance. According to the data shown in Fig. 2, changes in conductivity over four mold cycles are tolerably small, in which case we conclude that composite films produced after the first molding cycle are sufficiently uniform for further analysis.

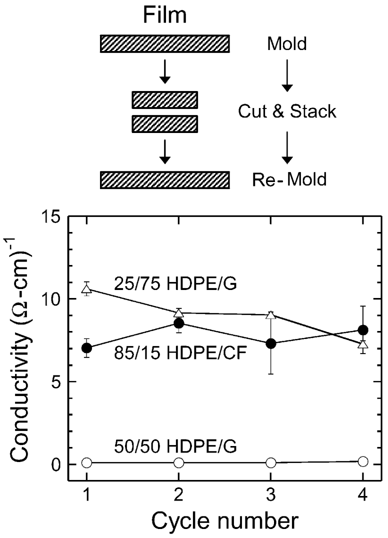

Fig. 2. Composite homogeneity and process reproducibility measured on the basis of electrical conductivity. As seen in the schematic illustration, samples have been cut in half, stacked and remolded to their original thickness during each cycle. Carbon fibers measuring 1.00 mm long (CF_1) have been used in these composites. Solid lines serve to connect the data.

3.2. Mixing/molding conditions and CFs

Mixing and molding of the HDPE/CF and HDPE/(G + CF) composites may have deleterious effects on the mechanical integrity of CF, often resulting in fiber breakage especially in high-aspect-ratio CF. To discern the magnitude of fiber breakage due to the dry-mixing step in the protocol adopted here, the CF has been separated from the HDPE–CF powder by placing the powder in water. Upon sedimentation, the higher-density CF is dried on a microscope slide. Carbon fibers have also been extracted from molded films by: (i) dissolving the HDPE in hot decalin; (ii) removing the fibers from the solvent; and (iii) again drying them on a microscope slide. The lengths of the CF have been measured by optical microscopy and are compared with the as-received fibers in Table 1. The average length reported in this table corresponds to 200 individual fibers in each composite.

The average length of the CF measuring 1.00 mm in

Table 1
Effect of mixing and molding on CF breakage

Specimen	Average length (mm)		
	As-received	After dry-mixing	After molding
Pure CF_1 (1.00 mm)	0.76 ± 0.13	0.30 ± 0.01	–
HDPE/CF_1 (95/5, w/w)	–	0.74 ± 0.09	0.60 ± 0.07
HDPE/CF_1 (90/10, w/w)	–	0.57 ± 0.05	0.55 ± 0.05
HDPE/CF_1 (85/15, w/w)	–	0.48 ± 0.03	0.40 ± 0.02
Pure CF_2 (0.25 mm)	0.24 ± 0.08	0.21 ± 0.03	–
HDPE/CF_2 (85/15, w/w)	–	0.23 ± 0.04	0.13 ± 0.01

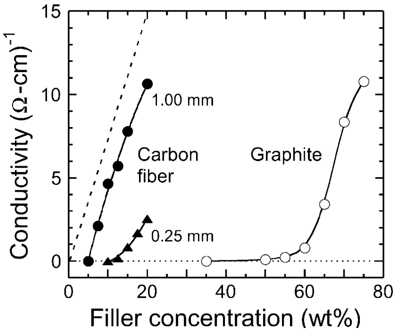

Fig. 3. Electrical conductivity of HDPE composites containing pure G or CF fillers. The first datum point in each data set represents zero (unmeasurable) conductivity, and the second datum point identifies the first measurable conductivity value. The dashed line represents predicted conductivities for randomly dispersed fibers according to Eq. (1), and the solid lines serve to connect the data.

length (CF_1) is found to be 24% less than the reported initial length. In marked contrast, the fibers measuring 0.25 mm in length (CF_2) are very close to their reported initial length. Processing the fibers in a mechanical mixer expectedly causes fiber breakage, the extent of which depends on fiber length and polymer/fiber ratio (mixing time and speed remain constant). The length of pure CF_1 decreases by 60% with respect to its original length after mixing, whereas the length of the shorter CF_2 is only reduced by 12% of its original length. Addition of HDPE to the powder results in less fiber breakage upon mixing, with the 95/5 (w/w) HDPE/CF_1 mixture displaying very little change in fiber length upon mixing. The molding process employed here also promotes additional fiber breakage, which is more pronounced for the shorter fibers than for the longer fibers. This counter-intuitive observation is attributed to the mold thickness, which is larger than the CF_2 length of 0.24 mm but smaller than the CF_1 length of 0.76 mm. Thus, the CF_2 fibers have a greater tendency to align parallel to the thickness direction of the mold and subsequently fracture when pressure is applied. The longer CF_1 fibers, on the other hand, tend to align in the plane of the mold and are less likely to fracture when pressure is applied.

3.3. Electrical conductivity

The variation in conductivity with respect to filler concentration is displayed in Fig. 3 for HDPE composites containing G and the two CF lengths. A feature of interest in this figure is the minimum filler concentration (expressed in wt%) that yields a measurable conductivity, which we designate as the threshold concentration. As anticipated, the composites containing the longest fibers (CF_1) exhibit the lowest threshold concentration at ~7.5 wt%, compared with ~12.5 wt% for the HDPE/CF_2 composites and ~50 wt% for the HDPE/G composites. High-aspect-ratio CF fillers possess the longest uninterrupted path for electrons, leading to higher conductivity at a given loading level. Graphite, however, consists of small primary particles that tend to aggregate into larger low-aspect-ratio clusters. It tends to disperse more evenly into the polymer matrix, thereby resulting in fewer particle–particle contacts at a given loading level and, consequently, a lower-conductivity polymer composite. As the filler concentration is increased beyond the threshold concentration, the conductivity of all the HDPE composites is observed to increase rapidly. The maximum conductivity of a conductive composite containing randomly oriented fibers can be estimated [51] from

$$\sigma_{\max} = \frac{2}{3\pi}\phi\sigma_{\mathrm{f}} \tag{1}$$

where ϕ and σ_{f} denote the volume fraction and conductivity of the fiber, respectively. Using the volume resistivity quoted by the supplier for σ_{f}, Eq. (1) yields the conductivity values identified by the dashed line in Fig. 3. The conductivities measured experimentally fall below this prediction, especially for the HDPE/CF_2 composites containing the shorter fibers. This disagreement is attributed to the presence of contact resistance between the CF, which is not considered in the derivation of Eq. (1). While the electron transport mechanism responsible for the conductivity of polymers filled with G or CF is still unclear, Dawson and Adkins [52] propose that the conductivity in CB-filled polymers (which are qualitatively similar to G-filled polymers) is regulated by *interparticle* electron transfer at low filler loadings and *intraparticle* electron transfer at high filler loadings.

Fig. 4 shows the conductivity of HDPE composites with various mixtures of G and CF at a constant total filler concentration (30 or 60 wt%). The conductivity of these HDPE/(G + CF) composites generally increases with (i) increasing filler concentration and (ii) increasing CF composition at a fixed total filler concentration. Composites without CF are good insulators, and composites with 30 wt% filler remain non-conductive until the CF content of the filler exceeds 30–50 wt%, depending on CF length. In

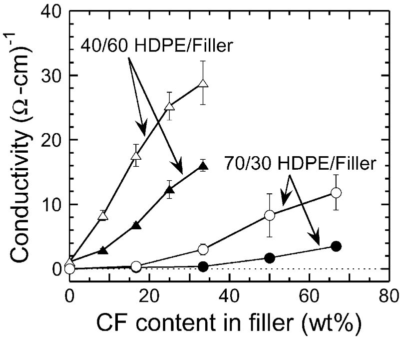

Fig. 4. Electrical conductivity of HDPE composites containing mixtures of G and CF. Each data set represents a constant total filler concentration (in wt%): 30 (circles) and 60 (triangles). The CF_1 (1.00 mm) and CF_2 (0.25 mm) fillers are designated by open and filled symbols, respectively. Solid lines serve to connect the data.

contrast, the conductivity of composites containing 60 wt% filler (which is above the threshold concentration of HDPE/G composites) increases rapidly upon addition of small quantities of CF. The conductivity of the HDPE/G composite with 50 wt% G is ~0.1 $(\Omega\text{cm})^{-1}$, whereas that of the HDPE/CF_1 composite with 10 wt% CF_1 is ~5.0 $(\Omega\text{cm})^{-1}$. Combination of these fillers to produce a 40/(50 + 10) HDPE/(G + CF) composite yields a jump in conductivity to almost 18 $(\Omega\text{cm})^{-1}$. This result clearly demonstrates that the conductivity of an HDPE/G composite above its threshold concentration can be significantly improved upon addition of small amounts of CF. Composites prepared with high G or CF loading levels possess high electron densities and small gaps between filler particles, which tends to induce high conductivity. Unfortunately, composite films containing more than 20 wt% CF overall are difficult to prepare and are visibly heterogeneous.

Addition of CF to HDPE/G composites increases the electrical conductivity due to bridging of G particles by CF. This bridging phenomenon increases the uninterrupted length of the conductive paths and the strength of the percolated filler network and, hence, the level of conductivity. Another feature evident in Fig. 4 is that, in all cases, improved conductivity is more pronounced for CF_1 than CF_2. Jana [53] has performed Hall effect measurements and finds that an increase in CF aspect ratio is accompanied by an increase in mobile carrier concentration. Hence, the effects of high mobile carrier concentration in CF_1 taken together with a high degree of bridging between filler particles combine to explain the high conductivity achieved in the HDPE/(G + CF_1) composites.

3.4. Morphological characteristics

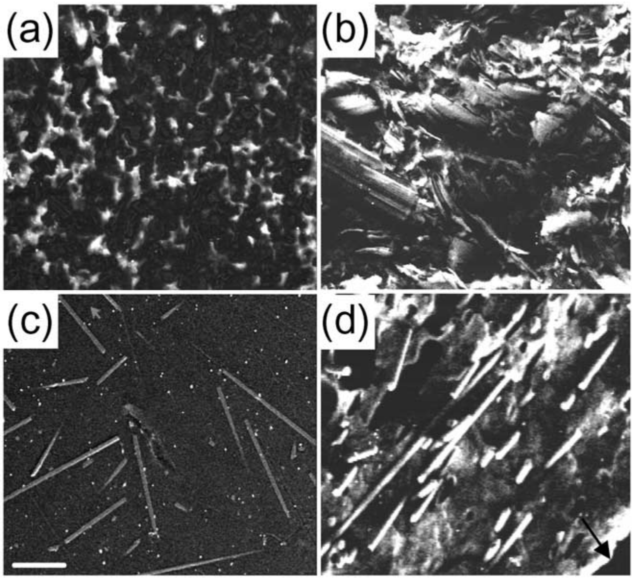

Fig. 5. Back-scattered electron micrographs of stained HDPE/G and HDPE/CF_2 composites near their threshold concentrations. The mold-contact surface and cross-fracture surface of a 50/50 (w/w) HDPE/G composite are shown in (a) and (b), respectively, whereas the mold-contact surface and cross-fracture surface of an 87.5/12.5 (w/w) HDPE/CF composite are displayed in (c) and (d), respectively. The scale marker displayed in (c) corresponds to 100 μm in (a) and (c) and 50 μm in (b) and (d). The arrow in (d) identifies a film surface.

A series of SEM micrographs obtained from stained samples of HDPE/G and HDPE/CF_2 composites are presented in Fig. 5. Recall that images are collected from sample surfaces in contact with the mold, as well as from cross-fracture surfaces. Micrographs of HDPE/G near the threshold concentration (Fig. 5a and b) reveal the existence of G particles exhibiting both short- and long-range connectivity in the plane and through the thickness of the composite film. Analogous images acquired from the HDPE/CF_2 samples (Fig. 5c and d) show that the fibers are primarily, but not exclusively, aligned in the specimen plane throughout the thickness of the sample. Fracture surfaces of composites containing either G or CF_2 exhibit the cleaved appearance typical of brittle failure. Higher resolution images of fractured HDPE/CF_2 composites provide evidence for clean fiber pullout during fracture, indicating weak HDPE–CF interfacial bonding.

3.5. Dynamic mechanical properties

The dynamic storage modulus (G') has been measured from 25 to 120 °C for all the composites examined here and does not show the existence of any thermal transitions over this range (recall that, according to the manufacturer, the melting point of the HDPE is 134 °C). Variation in the dynamic loss modulus (G'') is insignificant among the various samples, ranging from 10^8 to 10^9 Pa. For this reason and since G'' is relatively invariant over the temperature range examined, these data are not provided. Values of G' for the filled samples consistently lie in the range 10^9–10^{10} Pa and decrease at different rates as the melting temperature of HDPE is approached. The magnitude of G' obtained for neat HDPE at 25 °C (7×10^8 Pa) agrees well with the findings of Takayanagi and Sinnot [54], who report

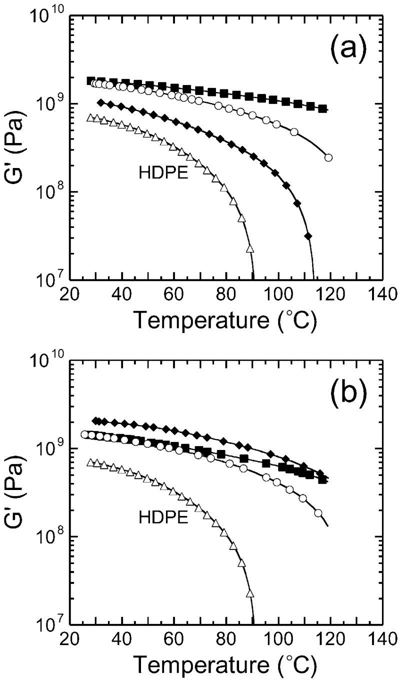

Fig. 6. The dynamic storage modulus (G') as a function of temperature for pure HDPE (△), as well as HDPE/G (▲), HDPE/CF_1 (■) and HDPE/CF_2 (○) composites, measured according to two different concentration criteria: (a) 15 wt% filler and (b) threshold concentrations (50 wt% G, 7.5 wt% CF_1, 12.5 wt% CF_2). Solid lines serve to connect the data.

a value of G' on the order of 10^9 Pa for HDPE at ambient temperature. Fig. 6a displays the temperature dependence of G' for HDPE/G and HDPE/CF composites with 15 wt% filler. All the fillers promote a small increase in G' near ambient temperature, but their primary effect is to improve the stiffness of the composites at higher temperatures. The temperature at which G' begins to decrease significantly occurs in the vicinity of 60 °C for pure HDPE, 100 °C for HDPE/G and 120 °C for HDPE/CF_2. Surprisingly, the modulus for HDPE/CF_1 remains high throughout the entire temperature range investigated. The mechanical reinforcing behavior of these samples corresponds well with their threshold filler concentrations as deduced from Fig. 2. At 15 wt% loading, the composite filled with CF_1 is well above its threshold concentration, whereas the sample filled with CF_2 is just above its threshold concentration, and the sample filled with G is well below its threshold concentration. Thus, the polymer composite possessing the most complete percolated filler network appears to exhibit the best high-temperature mechanical properties.

To discern the effect of filler percolation on mechanical property development in these HDPE composites, we next examine the composites at their threshold concentrations. According to the data provided in Fig. 6b, all three fillers yield remarkably similar mechanical properties at this condition (50 wt% G, 7.5 wt% CF_1 and 12.5 wt% CF_2). In this case, the sample containing G has a slightly higher G' than either of the CF composites, presumably due to its substantially higher filler concentration. The results presented in this figure suggest that the magnitude and temperature (T) dependence of G' for these HDPE composites depends primarily on the proximity of the filler loading level to the threshold concentration, rather than on the type or absolute concentration of the filler present. This conclusion is further supported by the data displayed in Fig. 7, which shows the variation of G' with respect to temperature for HDPE/CF composites containing 5, 10 and 15 wt% CF. This concentration range spans the threshold concentrations for both CF_1 and CF_2. The composites with 5 and 10 wt% CF_2 in Fig. 7a are below their threshold concentrations of 12.5 wt% CF_2, and they exhibit indistinguishable values of G' over the entire temperature range. The sample with 15 wt% CF_2 is above the threshold concentration and exhibits a slightly higher value of G' at low temperatures, but a markedly higher G' as the melting point is approached. Similar behavior is observed for the HDPE/CF_1 composites in Fig. 7b. In this case, the specimens with 10 and 15 wt% CF_1 lie above the threshold concentration of 7.5 wt% CF_1 and exhibit virtually identical and enhanced $G'(T)$ behavior relative to the HDPE/CF_1 composite with 5 wt% CF_1. Without exception, the HDPE/CF composites are much stiffer than pure HDPE over the entire temperature range investigated.

Values of G' measured at 30 and 100 °C for HDPE/(G + CF) composites are displayed in Fig. 8a and b, respectively. To permit comparison, the sample compositions are identical to those in Fig. 4, and the total filler content for

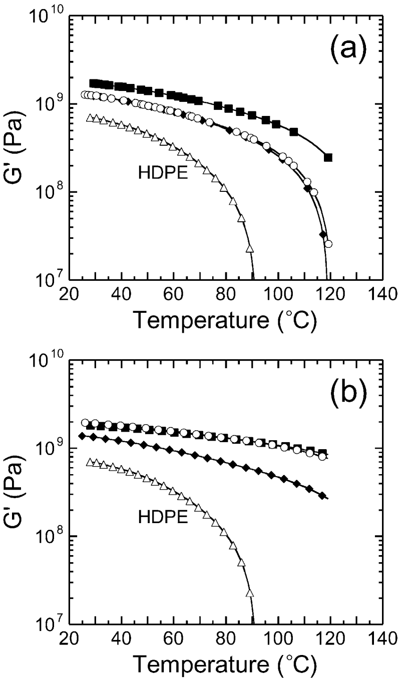

Fig. 7. Temperature and composition dependence of G' for (a) HDPE/CF_2 and (b) HDPE/CF_1 composites at four different filler concentrations (in wt%): 0 (△); 5 (▲); 10 (○); 15 (■). Solid lines serve to connect the data.

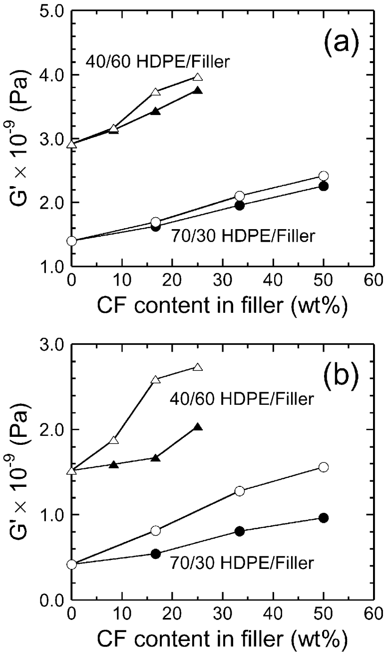

Fig. 8. Variation of G' with respect to filler composition and fiber length for HDPE/(G + CF) composites containing 30 and 60 wt% filler (circles and triangles, respectively) at (a) 30 and (b) 100 °C. The CF_1 (1.00 mm) and CF_2 (0.25 mm) fillers are designated by open and filled symbols, respectively. Solid lines serve to connect the data.

each data set is constant. At 30 °C, G' is significantly improved by increasing the overall filler concentration from 30 to 60 wt%, while increasing the length or concentration of CF in the filler has a less profound effect. In the composites with 30 wt% total filler concentration, G' ranges from 1.4×10^9 to 2.2×10^9 Pa when the CF content of the filler increases from 0 to 50 wt%. Similarly, G' ranges from 2.9×10^9 to 3.8×10^9 Pa when the CF content of the filler increases from 0 to 25 wt% at 60 wt% total filler concentration. In this case, an increase in CF composition at constant total filler content is accompanied by a reduction in the composition of G from above its threshold concentration to below its threshold concentration. Concurrently, the CF concentration increases from below to above its threshold concentration. These offsetting effects may explain the weak dependence of G' on CF content evident in Fig. 8a. At 100 °C (Fig. 8b), G' behaves in similar fashion with regard to CF composition, except that a marginally more pronounced reinforcing effect is apparent for the longer fibers relative to the shorter fibers at the same total filler concentration.

3.6. Thermal properties

While the G, CF and G/CF fillers serve to reinforce HDPE at elevated temperatures, the thermal properties of the HDPE matrix—e.g. the heat of fusion and melting and crystallization temperatures—are not affected significantly by their presence. Thus, a detailed description of the corresponding DSC data is not presented. The specific heat of fusion for all the filler types (including mixtures) and at all loading levels has been found to vary by less than 10% from the value for pure HDPE (210 J/g). We therefore conclude that the improved *stiffness* of our filled HDPE composites at elevated temperatures is not due to filler-induced changes in HDPE crystallinity. The largest effect on the transition temperatures occurs in the 85/15 (w/w) HDPE/CF_1 composite, which exhibits a mere 4 °C increase in melting temperature, as well as a 4 °C reduction in crystallization temperature, relative to pure HDPE. Transition temperatures do not change appreciably for HDPE/G or HDPE/(G + CF) composites with up to 50 wt% total filler.

4. Conclusions

This study has demonstrated that the addition of a second carbonaceous filler, such as CF, to HDPE/G composites improves their electrical conductivity and high-temperature mechanical integrity (as measured by G'). The observed increase in conductivity is more pronounced if the concentration of G is already above its threshold concentration. In this case, the conductivity of the composite has been found to jump from ~0.1 $(\Omega\text{cm})^{-1}$ at 50 wt% pure G and ~5.0 $(\Omega\text{cm})^{-1}$ at 10 wt% pure CF_1 to ~18.0 $(\Omega\text{cm})^{-1}$ when these two fillers are combined in a 40/(50 + 10) (w/w) HDPE/(G + CF) composite. This result confirms that the conductivity of an HDPE/G composite already loaded above its threshold concentration can be significantly improved upon addition of a reasonably small amount of CF. Optical and electron micrographs reveal that the G particles exhibit short- and long-range connectivity in the HDPE matrix, whereas CF may exhibit preferential alignment, depending on its length relative to the composite film thickness. The magnitude and temperature dependence of G' measured for HDPE/CF and HDPE/G composites are more sensitive to the proximity of the filler loading level to the threshold concentration than on the filler type or concentration. Addition of these fillers, as well as their mixtures, does not significantly alter the thermal properties of HDPE, in which case the observations reported herein can be attributed solely to the fillers employed. The reinforcing effect of long CFs is more pronounced at elevated temperatures below the melting point of the HDPE matrix.

Acknowledgements

The authors thank Mr A. Rieves (National Power Inc.) for providing the HDPE and graphite powder; Drs R.F. Davis, T. Hare and D.M. Maher (NCSU) for technical assistance; and Mr J.J. Semler for his suggestion of using carbon fiber/graphite mixtures.

References

[1] Narkis M, Ram A, Flashner F. Polym Eng Sci 1978;18:649.
[2] Narkis M, Ram A, Stein Z. Polym Eng Sci 1981;21:1049.
[3] Aminabhavi TM, Cassidy PE. Rubber Chem Technol 1990;63:451.
[4] Blaszkiewicz M, Mclachlan DS, Newnham RE. Polym Eng Sci 1992;32:421.
[5] Poulaert B, Issi JP. Polymer 1983;24:841.
[6] Fujikura Y, Kawarai M, Ozaki F. Polym J 1989;21:609.
[7] Miyasaka K, Watanabe K, Jojima E, Aida H, Sumita M, Ishikawa K. J Mater Sci 1982;17:1610.
[8] Kirkpatrick S. Rev Mod Phys 1973;45:574.
[9] Abeles B, Pinch HL, Gittleman JI. Phys Rev Lett 1975;35:247.
[10] Liang NT, Shan Y, Wang S-Y. Phys Rev Lett 1976;37:526.
[11] Yacubowicz J, Narkis M, Benguigui L. Polym Eng Sci 1990;30:459.
[12] Al-Allak HM, Brinkman AW, Woods J. J Mater Sci 1993;28:117.
[13] Bengtsson P, Kubat J. Plast Rubb Compos Proc Appl 1993;20:151.
[14] Moon TJ, Lee MK, Jeon IS, Shin YJ. Polym (Korea) 1995;19:789.
[15] Paul A, Thomas S. J Appl Polym Sci 1997;63:247.
[16] Mather PJ, Thomas KM. J Mater Sci 1997;32:401.
[17] Tang H, Chen XG, Luo YX. Eur Polym J 1997;33:1383.
[18] Chan C-M, Cheng C-L, Yuen MMF. Polym Eng Sci 1997;37:1127.
[19] Yang GC, Teng RR, Xiao P. Polym Compos 1997;18:477.
[20] Lee GJ, Suh KD, Im SS. Polym Eng Sci 1998;38:471.
[21] Lee JY, Lee GJ, Han MG, Suh KD, Im SS. Polym (Korea) 1998;22:625.
[22] Beaucage G, Rane S, Schaeffer DW, Long G, Fischer D. J Polym Sci B: Polym Phys 1999;37:1105.
[23] Foulger SH. J Polym Sci B: Polym Phys 1999;37:1899.
[24] Yu G, Zhang Q, Zeng HM, Hou YH, Zhang HB. Polym Eng Sci 1999;39:1678.
[25] Balabanov S, Krezhov K. J Phys D: Appl Phys 1999;32:2573.
[26] Rieker TP, Hindermann-Bischoff M, Ehrburger-Dolle F. Langmuir 2000;16:5588.
[27] Yi XS, Zhang JF, Zheng Q, Pan Y. J Appl Polym Sci 2000;77:494.
[28] Marr DWM, Wartenberg M, Schwartz KB, Agamalian MM, Wignall GD. Macromolecules 1997;30:2120.
[29] Oakey J, Marr DWM, Schwartz KB, Wartenberg M. Macromolecules 1999;32:5399.
[30] Oakey J, Marr DWM, Schwartz KB, Wartenberg M. Macromolecules 2000;33:5198.
[31] Karasek L, Meissner B, Asai S, Sumita M. Polym J 1996;28:121.
[32] Bottreau AM, Boutaudon A, Merzouki A. J Chim Phys–Chim Biol 1997;94:1568.
[33] Marquez A, Uribe J, Cruz R. J Appl Polym Sci 1997;66:2221.
[34] Kim D-J, Seo K-H, Hong K-H, Kim S-Y. Polym Eng Sci 1999;39:500.
[35] Ghosh P, Chakrabarti A. Eur Polym J 2000;36:1043.
[36] Wang YS, Ogurkis MA, Lindt JT. Polym Compos 1986;7:349.
[37] Ezquerra YA, Kulescza M, Baltacalleja FJ. Synth Met 1991;41:915.
[38] Cespedes F, Martinez Fabregas E, Alegret S. Trac-Trends Anal Chem 1996;15:296.
[39] Navarro-Laboulais J, Trijueque J, Garcia-Jareno JJ, Benito D, Vicente F. J Electroanal Chem 1998;444:173.
[40] Yi XS, Song YH, Zheng Q. J Appl Polym Sci 2000;77:792.
[41] Nagata K, Iwabuki H, Nigo H. Compos Interf 1999;6:483.
[42] Song YH, Pan Y, Zheng Q, Yi XS. J Polym Sci B: Polym Phys 2000;38:1756.
[43] Agari Y, Ueda A, Nagai S. J Appl Polym Sci 1994;52:1223.
[44] Pipe RB, MacCullough RL, Taggart DG. Polym Compos 1982;3:34.
[45] Bozart MJ, Gilles Jr JW, MacCullough RL. Polym Compos 1987;43:1117.
[46] Wang GQ, Zeng P. Polym Eng Sci 1997;37:96.
[47] Vilcakova J, Saha P, Kresalek V, Quadrat O. Synth Met 2000;113:83.
[48] Calleja FJB, Bayer RK, Ezquerra TA. J Mater Sci 1988;23:1411.
[49] Sawyer LC, Grubb DT. Polymer microscopy. New York: Chapman & Hall, 1987. p. 102.
[50] Kanig G. Colloid Polym Sci 1983;261:373.
[51] Bylthe AR. Electrical properties of polymers. Cambridge: Cambridge University Press, 1980. p. 126.
[52] Dawson JC, Adkins CJ. J Phys: Condens Matt 1996;8:8321.
[53] Jana PB. Plast Rubb Compos Proc Appl 1993;20:107.
[54] Takayanagi M, Sinnot J. In: Ward IM, editor. Mechanical properties of solid polymers, 2nd ed. New York: Wiley, 1983. p. 180–6.